

## Structural Form-Finding of Multi-Span Undulating Funicular Beam Structure

Hua CHAI<sup>\*,a</sup>, Mohammad BOLHASSANI<sup>c</sup>, Masoud AKBARZADEH<sup>a,b</sup>

<sup>\*,a</sup> Polyhedral Structures Laboratory, Weitzman School of Design, University of Pennsylvania, Philadelphia, USA  
Pennovation Center, 3401 Grays Ferry Ave. Philadelphia, PA, 19146

<sup>b</sup>General Robotic, Automation, Sensing and Perception (GRASP) Lab, School of Engineering and Applied Science, University of Pennsylvania, Philadelphia, USA

<sup>c</sup>The Bernard and Anne Spitzer School of Architecture, The City College of New York, New York, USA

### Abstract:

The recent innovation of building structure has been widely developed on generating funicular systems. The proposed strategy significantly reduces material usage compared to conventional concrete constructions. This paper presents a form-finding method that allows the user to design the integrated undulating beam system using graphic statics. By applying the method of the Geometric Degrees of Freedom, the modular units can span in multiple directions, iterating the boundary condition within the network to generate compression-only to compression-tension combined structures. It results in an undulating shape of the beam with various thicknesses that can integrate the necessary building services such as an energy heating – cooling system. The average thickness is significantly saved through the process (Figure 1). The preliminary structural analyses of a strip of the beam have shown the efficiency of the system compared with the traditional construction systems. Additionally, the post-tensioning cables are designed to be embedded within the structure to minimize the reinforcement.

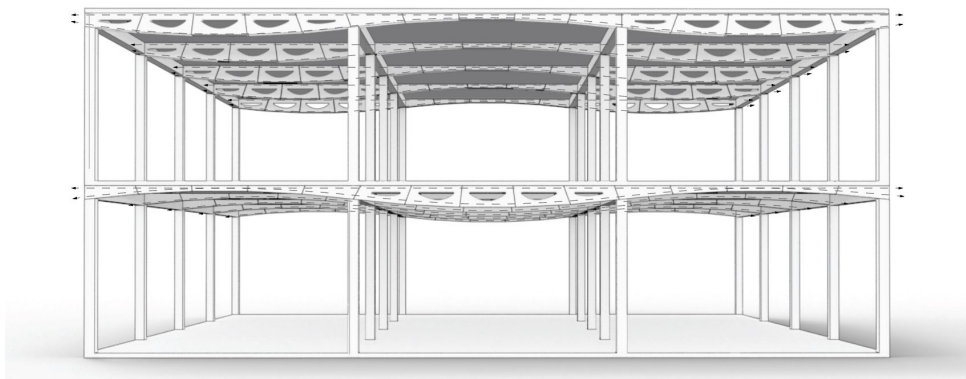


Figure 1: Two stories multi-span undulating funicular beam structure with embedded post-tensioning cables.

**Keywords:** graphic statics, beam design, form-finding, additive manufacturing

## **1. Introduction**

As the essential artificial material, concrete has been widely applied to the modern building industry to transform construction and preserve the human quality of life. From the structural perspective, it is built with a high compressive loads capacity and solid resistance to punching shear forces. However, the AEC sector, including concrete, contributes to a variety of global environmental problems, such as air and water pollution, waste production. Concrete has an enormous carbon footprint, explicitly from cement production [1]. The US government record shows over 600M tons of material waste generated from the daily construction and demolition in 2018 [2]. The number is growing every year. It is imperative to reduce the amount of material used and establish a more sustainable strategy for design practice.

Recently, by designing and analyzing the structure of the generated geometry, various promising research maximized the material efficiency technically and economically. Utilizing the topological optimization method to generate floor-slab, the research team investigated the additive fabrication constraints to further optimize the geometry for Binder Jet 3D printing with fiber-reinforced concrete [3]. The prefabricated discrete funicular floor components are developed to realize the structural efficiency and flexibility of the 3D-printing technique. The system is constructed with external tension ties that connect the supports to absorb horizontal forces [4]. The reusable formwork is designed with precisely controlled 3D printed concrete to expertise the fabrication process. The automotive workflow requires less labor, and the modular prototype delivers high customizability [5]. Another reusable strategy is focusing on the demolished concrete. Instead of grinding to rubble, the concrete walls can be divided into multiple pieces and cut precisely to be transferred as segments. It can be used in other construction, such as a pedestrian bridge [6]. Reconsidering the conventional concrete casting process, the pre-defined void areas with infilling PET bottles can also reduce material usage. This design investigation explored the potential of the local construction needs and the availability of manufacturing techniques [7].

### **1.1. Contributions**

All the well-established research has proved the feasibility of the optimized floor system using both casting concrete and additive manufacturing. In this paper, we present a form-finding method that allows the user to design the integrated multi-span undulating beams. The post-tensioning cable is embedded in the structure to minimize the reinforcement. Therefore, the geometry can be segmented as modular components directly fabricated by concrete 3D printing. The depositing process is designed to have as less material as possible and bought to the site in the first place without any formwork being produced.

## **2. Methodology**

We present the design methods based on developing the geometric operations for the provided components. The structure is generated to take advantage of the capacity of graphic statics to perform in both compression and tension. Moreover, the post-tensioning cables are inserted through the designated voids in each segment.

### **2.1. Form finding**

In this section, we demonstrate the form-finding method with the optimized geometry. The goal is to determine a flexible, continuous system to be implemented in different design schemes. Such a process is conducted through the method of Geometric Degree of Freedom and structural form-finding process. The user can parameterize it to further by adjusting the depth and span of the beam.

We will explain the methodology mainly utilizing the 2D graphic statics implementation. It helps the designer to understand the relationship between the forces and corresponding resultants. Moreover, it is not only working with 2D scenarios. The method can be extended to 3D and has been developed through multiple projects. 3D/polyhedral graphic statics was first introduced by Rankine and Maxwell [8, 9]. The intensive related research and studies have explored the potential of a design application with various material types [10–15]. Range from sheet-based material to spatial funicular concrete geometry, the polyhedral graphic statics provide an intuitive geometric method to generate complex, efficient structures.

### 2.1.1. Geometric degree of freedom

Starting with the initial structure generated by 2D graphic statics, Figure 2b presents the compression-tension combined structure with four apply loads and two reaction forces. The purpose of Geometric Degrees of Freedom (GDoF) is to manipulate the geometry without breaking the *force* diagram.

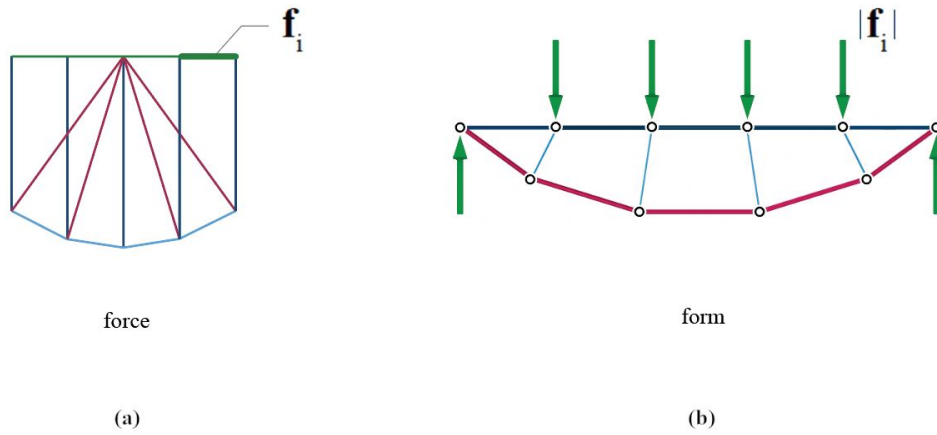


Figure 2: (a) force diagram; (b) form diagram - tension and compression combined structure.

For a single polygon, by choosing the length of  $l_1$ , the other edges' length depends on the length of  $e_i$  in Figure 3b. It shows that the length of edge 2 and edge 12 changed along with edge  $e_i$ . This chosen edge is often referred to as *independent edges*, and the rest of the edges can be referred to as the *dependent edges* since they follow the dependent edges in completing the polygon. The Geometric Degrees of Freedom of a polygon is, in fact, the number of independent edges ( $e_{ind}$ ) whose various lengths give a family of polygons with parallel edges compared to the initial polygon.

$$GDoF = e_{ind} \quad (1)$$

The same concept can be extended to a network of 2D or 3D polygonal faces. Similar to the case of a single polygon, there are multiple edges on a network that can be chosen independently to complete a similar network with different edge lengths. The GDoF of a single polygon is equal to  $e - 2$  where  $e$  is the number of edges.

$$GDoF = e_{ind} \geq e - 2f \quad (2)$$

where  $e$  is the number of edges, and  $f$  is the number of polygonal faces of the network. Equality applies for simple cases in 2D but does not work in very complex scenarios. Inequality 2 can be rewritten in

terms of the faces of the network:

$$GDoF = e_{ind} \geq \sum_i^n (e_{f_i} - 2) - e_{sh} \quad (3)$$

where  $e_{f_i} - 2$  is the GDoF of the  $i$ -th polygon/face, and  $e_{sh}$  is the number of shared edges between the faces of the graph.

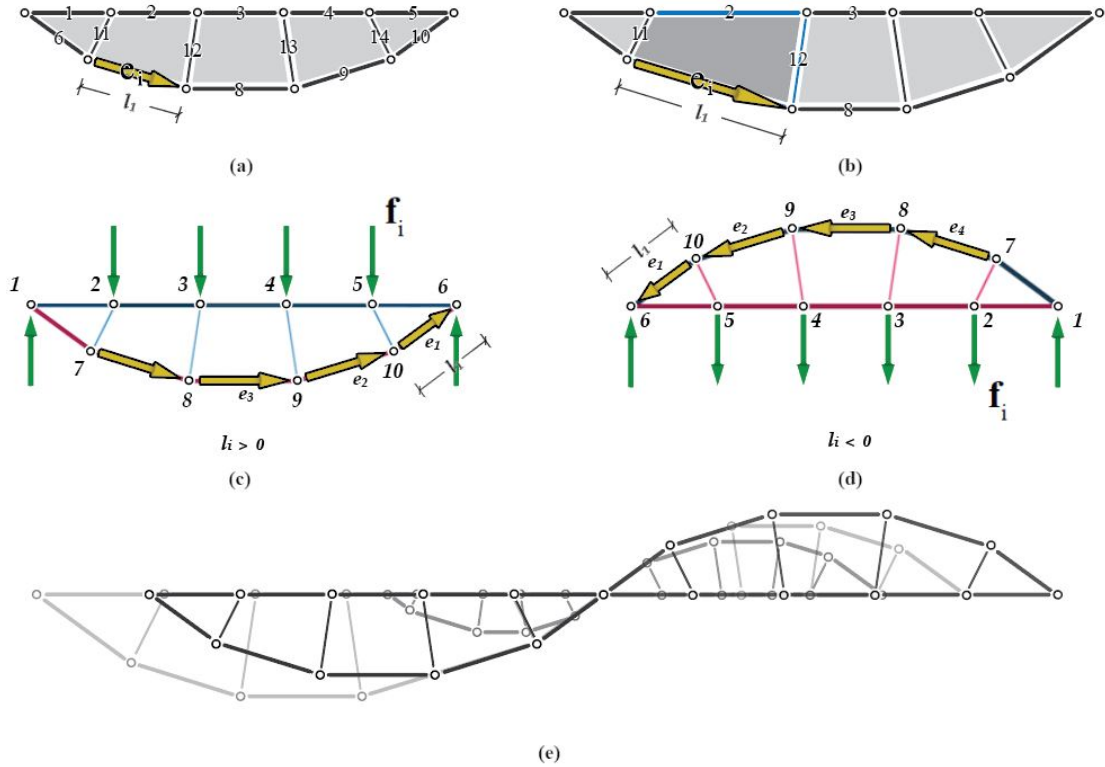


Figure 3: (a) 14 edges are defined in form diagram; (b) The design changes when edge length increases ; (c) (d) Two primary design schemes based on the length direction of the edge 1 ; (e) Different forms can be created through GDoF.

When manipulating the length of the edges, the direction plays a significant role in generating the design. We can define one direction as the positive length which is  $l_1 > 0$ , the other direction will be  $l_1 < 0$ . Figure 3cd illustrates the two main types of the design based on the length of  $l_1$ . Therefore, the overlapped diagram shown in Figure 3e describes the different variations.

### 2.1.2. Transformed modules

When the base module is constructed, the main task is to attach the two forms as the one continuous structure. Indeed, simply connecting the two ends of the modules is not the proper way to generate the system. For generating the beam, the top surface is considered to be flat to hold the floor slab. However, Figure 4 illustrates the end-to-end connection adding the extra volumes that vastly increase the thickness of the beam. The result is introducing more material usage eventually, which is not the purpose of the

design. So this point-to-point connection needs to be reconsidered, and we developed the manipulation of shifting the support locations for further development.

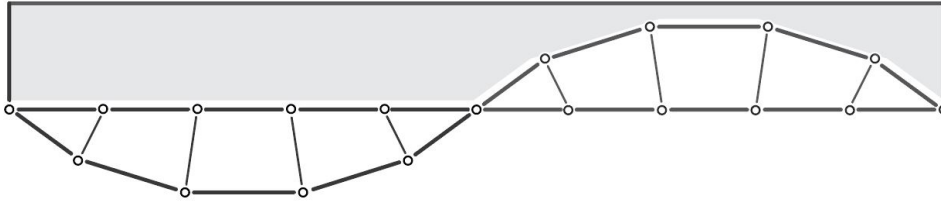


Figure 4: Extra space required (grey color) to design the beam using the end-to-end connection.

First, the end node for both modules needs to be removed, and the resultant forces have to be transferred to keep the structure equilibrium. The internal forces of the member connecting the last node are shown in Figure 5c. There are two adjacent nodes, the top one with applied load is under compression, and the other one below has the force pulling away from the node, so it is under tension. When the forces are clearly defined from the original form diagram, the next step is removing the members and preserving the previous internal forces. So the forces are now transferred as the reaction forces for the new form diagram (Figure 5d).

The force diagram indicates the transition of the removing process (Figure 5b&e). It is adjusted from the single force at both ends with force edge parallel to apply loads to dual forces. The green color represents the global forces since the applied loads stay the same, so the only factor changing is the reaction forces. The normal of edges based on the right-hand rule in the force diagram also present the force directions matched with the original internal forces. Therefore, the edges shown in red are related to tension members in the form diagram, eliminating the end node and resulting in the edge being switched to be part of global forces. The final form is realized as the new prototype to be tested in the following sections.

### 2.1.3. Selecting schemes

For instance, in Figure 6, the same process that manipulates the length of  $l_1$  in both directions generates six different types of forms. The distinction between the previous operation and the current GDoF process is that  $l_1$  can control the height of the structure. The edges can be flipped to the other side instead of only expanding horizontally. By vanishing the endpoint for both ends, the triangle connection is removed, and it adds an extra level of freedom when applying GDoF. Moreover, it provides more options for the design selection.

In general, adjusting the length of  $l_1$  is the solution to define the proper position of the edges in the form diagram. The selection process needs to consider the overall constraints and the design requirement. For creating the undulating system, the top surface of the beam structure is used to hold floor slabs, so any curved member will not be a suitable option. Additionally, when combining the two modules to form the one continuous system, the thickness is also an important factor to be reflected in the design.

Based on the above conditions, the overall satisfied form can be selected as Figure 6c1&d3. The flat members are at the top for carrying the live loads of the floor slabs. Furthermore, the bottom part can be aligned for the potential cable connections.

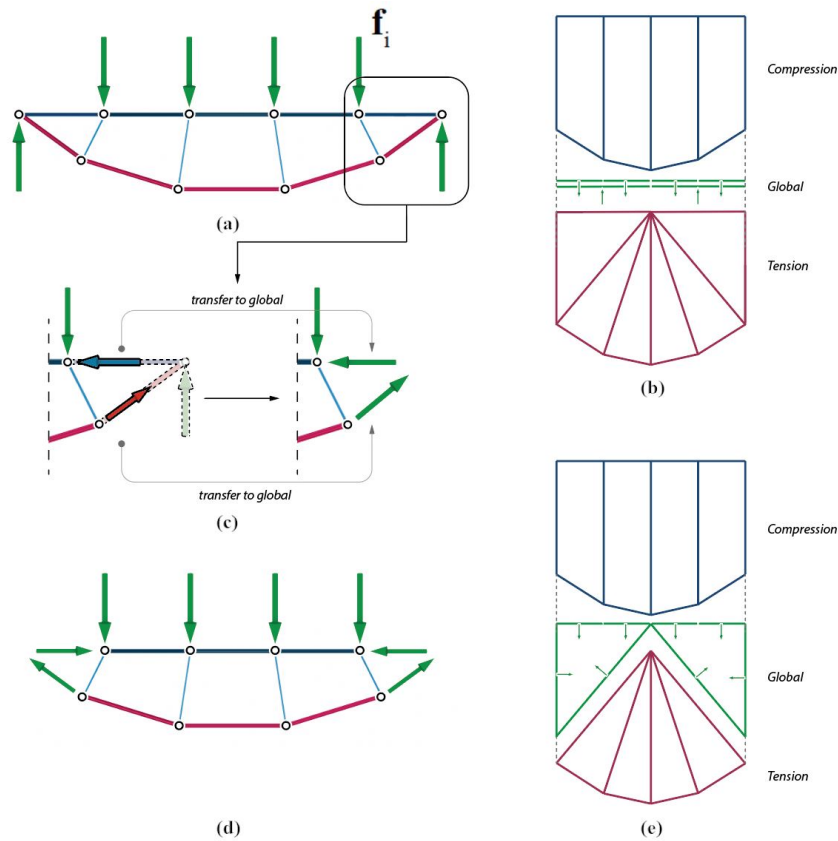


Figure 5: (a) Original form diagram; (b) Original force diagram; (c) Removing last node and transferring the global forces; (d)(e) Updated form & force diagram.

#### 2.1.4. Generating undulating Funicular Beam

The last step is to demonstrate the joint logic of the updated modules. In Figure 7, we can see that node 4 and node 8 is the last node for both schemes. Because the unit is symmetrical, overlapping them will create an undulating structure that can span in both directions. Then the next problem is to solve the forces that were initially attached to the members, especially the global forces.

When the nodes are merged, the reaction forces have to be recalculated (Figure 7). The horizontal forces will cancel each other out, and only the vertical forces need to be replaced by the columns. Figure 7 illustrates the potential location for the vertical supports.

#### 2.1.5. Geometric optimization

The initial shape of the structure is defined from the force diagram. The advantage of using graphic statics is when manipulating the parameter in the force diagram, the equilibrium form will be determined simultaneously. Figure 9 describes the possible geometries that can be generated by changing the curvature of the bottom curve (shown in red dash). All the edges besides the applied loads are connected to it. The angle and length of the mid-members obtain the changeable result that also affects the shape of the structure overall. From the practical aspect, the tensile member is better assigned with constant forces for materialization.

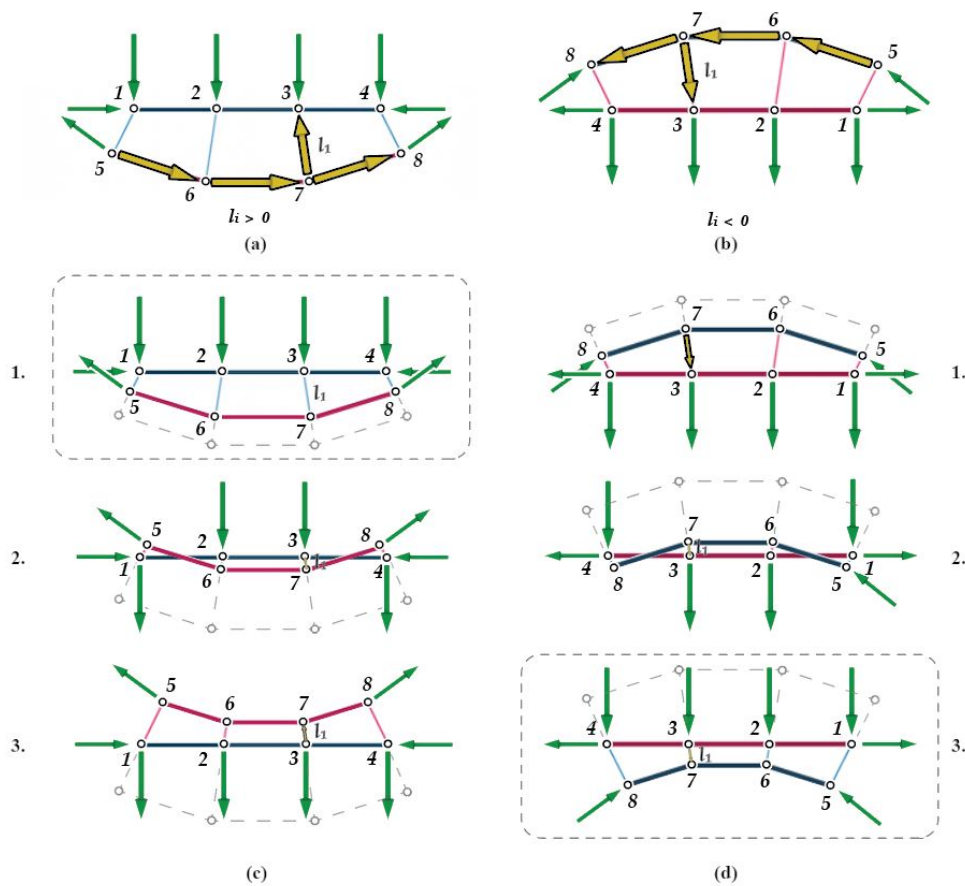


Figure 6: (a) GDoF when  $l_1 > 0$ ; (b) GDoF when  $l_1 < 0$ ; (c)(d) Corresponding design options related to the direction of edge 1.

By analyzing the level of curvature, forces in the form diagram correspond to the length of the force diagram. In general, if we assume the base unit is equal to the length of the applied load as 1kN. Then the rest edges will have the proper indicated force number related to the applied forces. In order to maintain the constant forces for the same cable running through, the curve needs to be replaced with a circular arc, so the length of the edges that correspond to the tension members are equal.

### 3. Structural performance

In order to study the structural performance of the bridge, a displacement control analysis by applying displacement on 1 foot next to the middle column was performed. The top and bottom cords are both post-tensioned (standard 133 kN, or 30kip). As it can be seen from the results, under the self-weight and applied displacement, the average stress in the units is around 14Mpa which is almost a quarter of the strength of the concrete (60Mpa). The maximum sliding of the middle part is 9.7mm (Figure 10).

### 4. Conclusion and future directions

In this paper, we explained how to design the undulating funicular beam system using the GDoF. The initial form is generated from 2D graphic statics, then through geometric manipulation to increase the level of freedom to construct the updated modules. Furthermore, when merging the two units together,

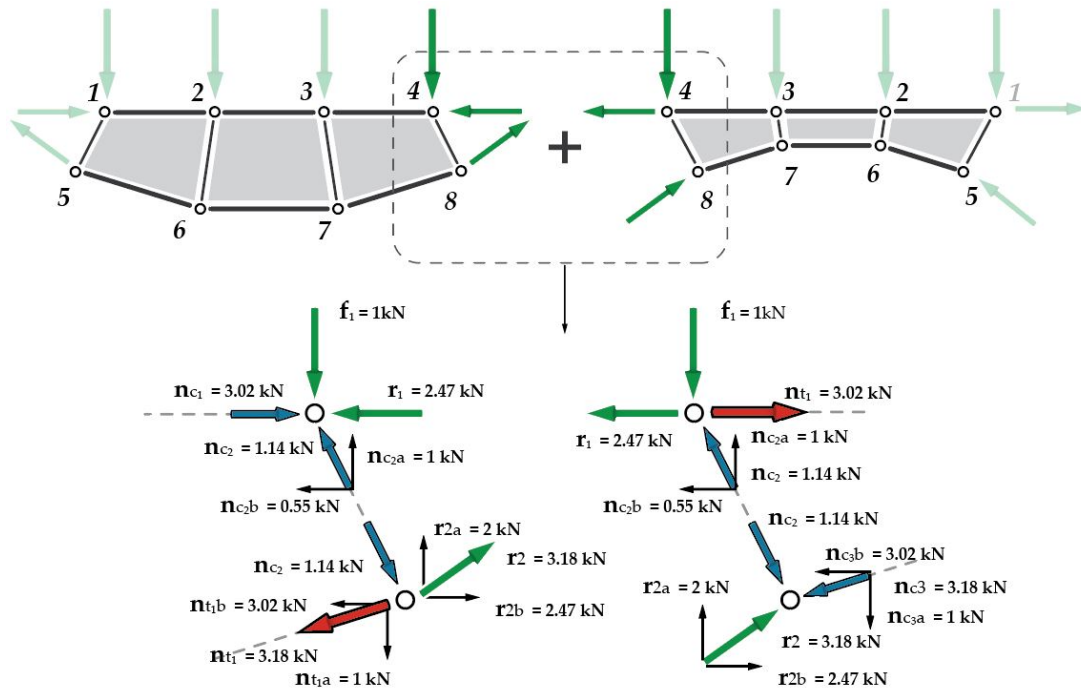


Figure 7: Merging nodes 4 and nodes 8 from two modules; the force distribution for locating the columns.

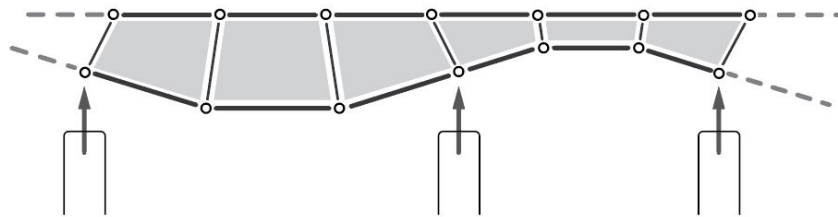


Figure 8: Column location for the continuous beam system.

the detailed force distribution is implemented to locate the column. For the future study, we will test the concrete printing for the one segment as the Figure 11 presented. The voids in the middle are designed with the limitation of printing overhangs. Lastly, the current beam design can be further developed to the floor structure by applying polyhedral graphic statics.

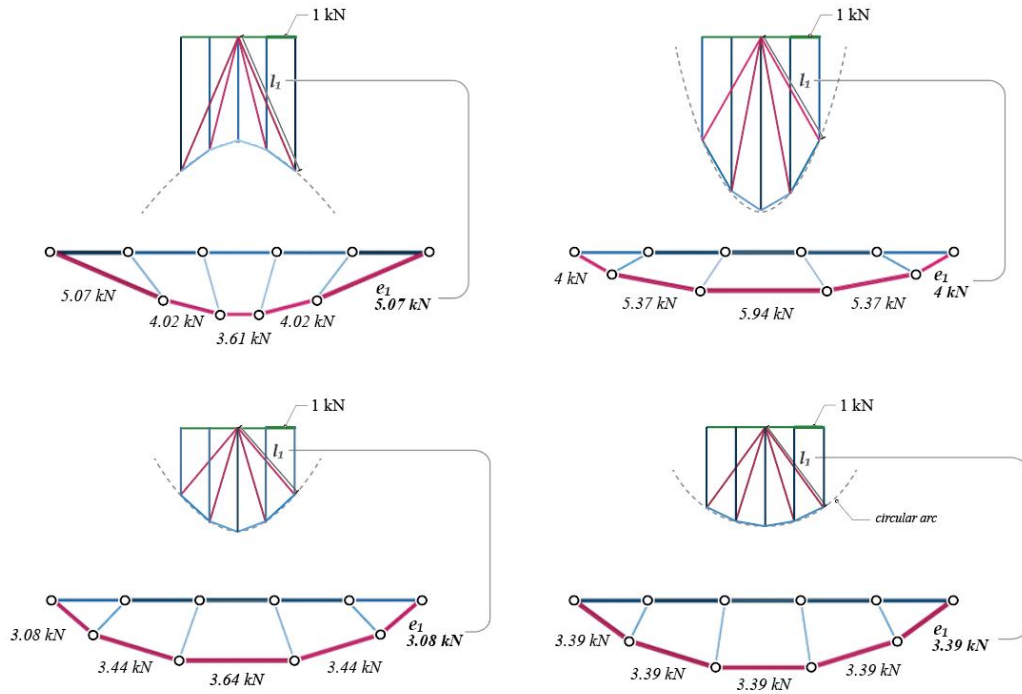


Figure 9: Optimization process for applying post-tensioning cables to maintain the constant forces.

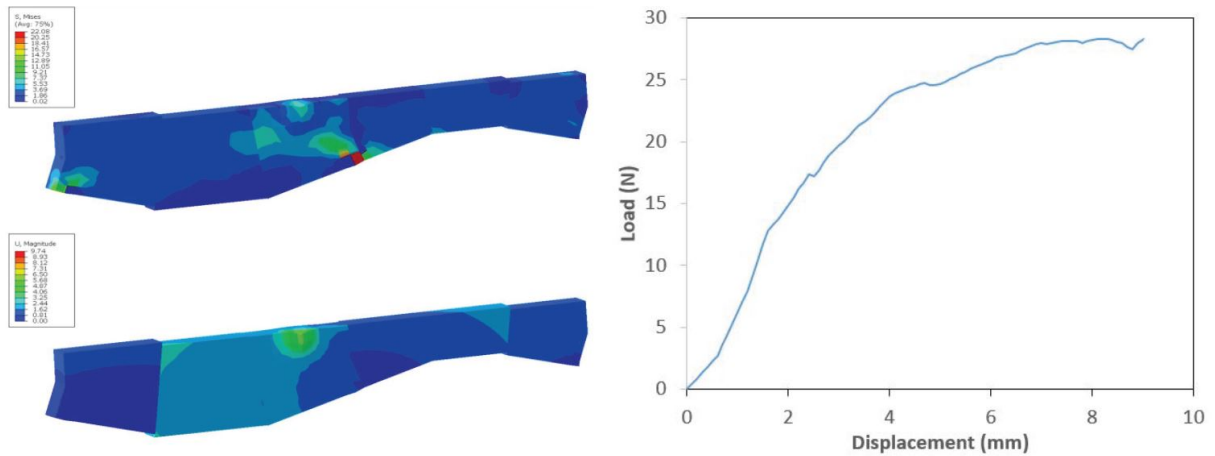


Figure 10: Stress, displacement and load-displacement curve of the prototype units.

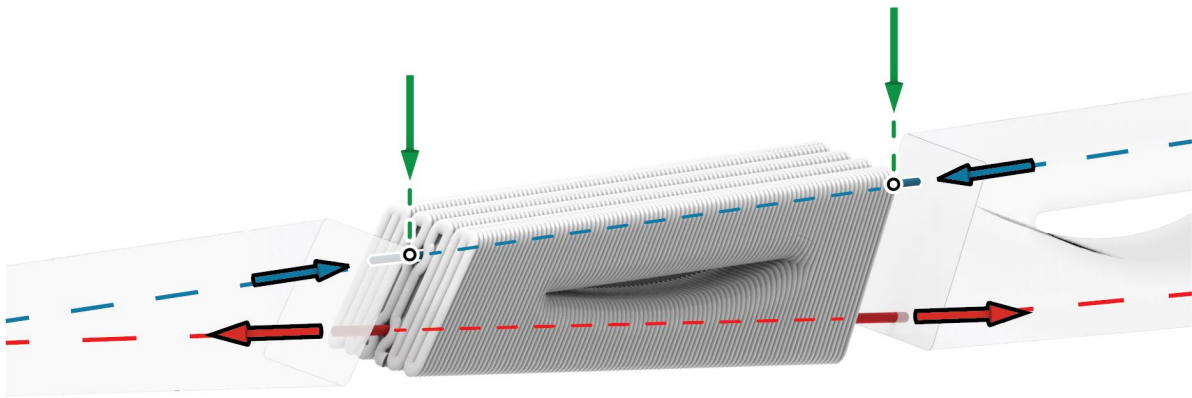


Figure 11: Simulated infills and printed layer for one segment.

## References

- [1] L. Ellis, A. Badel, M. Chiang, and Y.-M. Chiang, “Toward electrochemical synthesis of cement—an electrolyzer-based process for decarbonating  $\text{CaCO}_3$  while producing useful gas streams.,” *Proceedings of the National Academy of Sciences*, vol. 117, 2020.
- [2] United States Environmental Protection Agency, “Sustainable management of construction and demolition materials,” 2021. <https://www.epa.gov/smm/sustainable-management-construction-and-demolition-materials>, Last accessed on 2022-06-20.
- [3] A. Jipa, M. Bernhard, M. Meibodi, and B. Dillenburger, “3d-printed stay-in-place formwork for topologically optimized concrete slabs,” *TxA Emerging Design + Technology*, 2016.
- [4] P. Block, M. Rippmann, and T. Van Mele, “Compressive assemblies: Bottom-up performance for a new form of construction,” *AD Architectural Design*, vol. 87, pp. 104–109, July/August 2017. Special issue S. Tibbits (Ed.) - Autonomous Assembly: Designing for a new era of collective construction.
- [5] A. Anton, A. Jipa, R. Lex, and B. Dillenburger, “Fast complexity - additive manufacturing for bespoke concrete slabs,” *Association for Computer Aided Design in Architecture Conference*, 2020.
- [6] Structural Xploration Lab, “Reuse of cut concrete,” 2021. <https://www.epfl.ch/labs/sxl/index-html/research/reuse-of-concrete/>, Last accessed on 2022-06-20.
- [7] M. Ismail and C. T. Mueller, “A platform of design strategies for the optimization of concrete floor systems in india,” *International Conference of Structures and Architecture*, 2019.
- [8] W. J. M. Rankine, “Principle of the Equilibrium of Polyhedral Frames,” *Philosophical Magazine Series 4*, vol. 27, no. 180, p. 92, 1864.
- [9] J. C. Maxwell, “On Reciprocal Figures and Diagrams of Forces,” *Philosophical Magazine Series 4*, vol. 27, no. 182, pp. 250–261, 1864.
- [10] M. Akbarzadeh, M. Mahnia, R. Taherian, and A. H. Tabrizi, “Prefab, Concrete Polyhedral Frame: Materializing 3D Graphic Statics,” in *Proceedings of the IASS Annual Symposium 2017, “Interfaces: architecture . engineering . science”* (M. G. Annette Bögle, ed.), (Hamburg, Germany), September 2017.
- [11] Y. Lu, M. Cregan, P. A. Chhadeh, A. Seyedahmadian, M. Bolhassani, J. Schneider, J. R. Yost, and M. Akbarzadeh, “All glass, compression-dominant polyhedral bridge prototype: form-finding and fabrication,” in *Proceedings of IASS Symposium and Spatial Structures Conference 2020/21, Inspiring the next generation*, (Guildford, UK), August 23-27 2021.
- [12] Y. Lu, A. Seyedahmadian, P. A. Chhadeh, M. Cregan, M. Bolhassani, J. Schneider, J. R. Yost, G. Brennan, and M. Akbarzadeh, “Funicular glass bridge prototype: design optimization, fabrication, and assembly challenges,” *Glass Structures Engineering*, vol. 8, pp. 261–272, 2022.
- [13] M. Akbari, A. Mirabolghasemi, M. Bolhassani, A. Akbarzadeh, and M. Akbarzadeh, “Strut-based cellular to shellular funicular polyhedral materials,” *Advanced Functional Materials*, p. 2109725, 2022.

- [14] M. Akbari, M. Akbarzadeh, and M. Bolhassani, “From polyhedral to anticlastic funicular spatial structures,” in *Proceedings of IASS Symposium*, 2019.
- [15] M. Akbari, A. Mirabolghasemi, H. Akbarzadeh, and M. Akbarzadeh, “Geometry-based structural form-finding to design architected cellular solids,” in *Symposium on Computational Fabrication*, pp. 1–11, 2020.